Journal of Materials Chemistry A

REVIEW

View Article Online
View Journal | View Issue

Cite this: J. Mater. Chem. A, 2015, 3, 17497

Recent advances in critical materials for quantum dot-sensitized solar cells: a review

Jialong Duan,†[ab] Huihui Zhang,†[b] Qunwei Tang,*[ab] Benlin He[b] and Liangmin Yu*[ac]

Received 5th May 2015
Accepted 29th June 2015

DOI: 10.1039/c5ta03280f

www.rsc.org/MaterialsA

Quantum dot-sensitized solar cells (QDSCs) present promising cost-effective alternatives to conventional silicon solar cells due to their distinctive properties such as simplicity in fabrication, possibility to realize light absorption in wide solar spectrum regions, and theoretical conversion efficiency up to 44%. This review highlights recent developments in critical materials including quantum dots, photoanodes, counter electrodes (CEs), and electrolytes for QDSC applications. Among them, electron recombination at the photoanode/electrolyte interface limits the evolution of high-efficiency QDSCs, therefore the optimized construction of quantum dots, the various microtopographies of wide bandgap semiconductors (TiO_2, ZnO) as well as emerging CEs having good electrocatalytic activity are elaborated in this paper. We argue that these key factors can provide design guidelines for future successful applications and significantly promote the development of QDSCs. Liquid, quasi-solid-state, and solid-state electrolytes for QDSCs are summarized, aiming at enhancing the long-term stability of QDSCs. This review presented below gives a succinct summary of materials for QDSC applications, with a conclusion and future prospects section.

1. Introduction

1.1 Advances in quantum dot-sensitized solar cells (QDSCs)

The development of renewable energy sources is an urgent task to solve the emergence of global warming and emission of greenhouse gases.[1] In pursuit of cost-effectiveness, easy fabrication, and environmentally friendly energy, photovoltaic (PV) technology converting solar energy to electricity is a promising strategy as a solution to retard the energy crisis.[2] In 1991, a novel sandwich construction of the so-called dye-sensitized solar cell (DSSC) containing a dye-sensitized mesoporous photoanode, a liquid electrolyte having I^-/I_3^- redox couples, and a counter electrode (CE) was pioneeringly proposed by O'Regan and Grätzel.[3] This cell structure has attracted considerable attention over the past 24 years because of the advantages of its potential roll-to-roll fabrication procedure, cost-effective materials and manufacturing, and high energy conversion efficiency. Until now, a maximum power conversion efficiency of 13% has been recorded for optimized DSSCs.[4] However, the high cost and fussy synthesis procedures of organic dyes along with limited solar-to-electric conversion efficiency restrict the commercialization of DSSCs. Thus, solar cell devices using quantum dots (QDs) as sensitizers to substitute organic dyes are considered as promising alternatives to DSSCs. As shown in Fig. 1, the rapid growth of the number of research papers over the last 11 years demonstrates that semiconductor QDSCs as a branch of DSSCs are becoming one of the most promising devices on the stage of the PV market.

QDs, a class of narrow bandgap semiconductors, possess several excellent properties such as tunable bandgaps due to the quantum confinement effect,[5] higher absorption coefficients

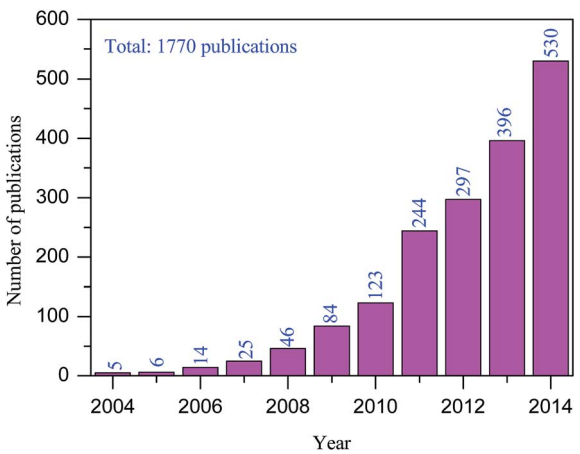

Fig. 1 Number of research articles published per year obtained from a simple and limited literature search using the keywords "quantum dot-sensitized solar cell" (data source: ISI Web of Knowledge).

[a]Key Laboratory of Marine Chemistry Theory and Technology, Ministry of Education, Ocean University of China, Qingdao 266100, P. R. China. E-mail: tangqunwei@ouc.edu.cn; yuyan@ouc.edu.cn; Fax: +86 532 66782533; Tel: +86 532 66782533

[b]Institute of Materials Science and Engineering, Ocean University of China, Qingdao 266100, P. R. China

[c]Qingdao Collaborative Innovation Center of Marine Science and Technology, Ocean University of China, Qingdao 266100, P. R. China

† The authors have equal contributions.

than most organic dyes,[6] and multiple exciton generation (MEG).[7] The scheme of MEG and the relationship between the bandgap and size are shown in Fig. 2. Using PbSe QDs to expound, herein, when irradiating PbSe QDs with photon energies greater than 2 times the QD bandgap, a multiplication of carrier extraction is rather obvious. Meanwhile, the absorption of PbS QDs can be changed from 680 to 1750 nm with the size increasing from 2.6 to 7.2 nm.[8] Based on the above merits, it is possible to realize the light absorption in the whole solar spectrum region *via* harvesting underutilized ultraviolet and currently unutilized infrared by means of combining several types of QDs.[9] Moreover, a direct bandgap semiconductor offers a stronger absorption coefficient of $\sim 10^4$ cm^{-1} and QDs can generate multiple electron–hole pairs from a single incident photon absorption in QDs, which lead to the maximum theoretical conversion efficiency up to 44%.[10]

On the other hand, QDs can be easily deposited on the surface of TiO_2 at room temperature by solution processed techniques such as successive ionic layer-by-layer adsorption and reaction (SILAR),[13] chemical bath deposition (CBD),[14] surface attachment through molecular linkers between optimized QDs and TiO_2,[15] spin coating,[16] electrodeposition and electrophoretic deposition (Fig. 3).[17,18] The techniques are facile and can be used in large scale production. This significantly reduces the consumption of energy to manufacture solar cells and gives the opportunity to realize industrialization. In this

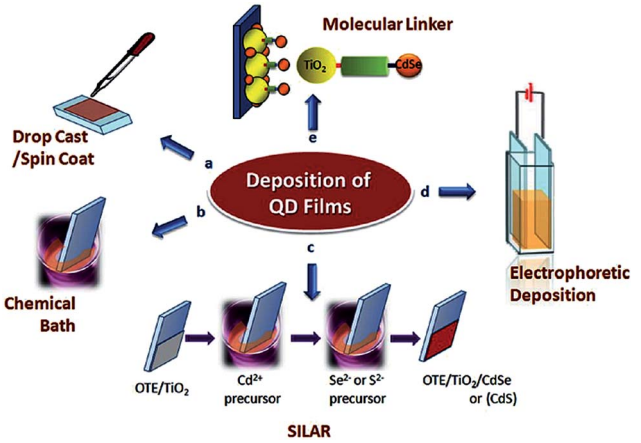

Fig. 3 Various approaches of depositing a QD suspension on electrode surfaces: (a) drop-casting or spin coating, (b) CBD, (c) SILAR, (d) electrophoretic deposition, and (e) a bifunctional linker approach.[19]

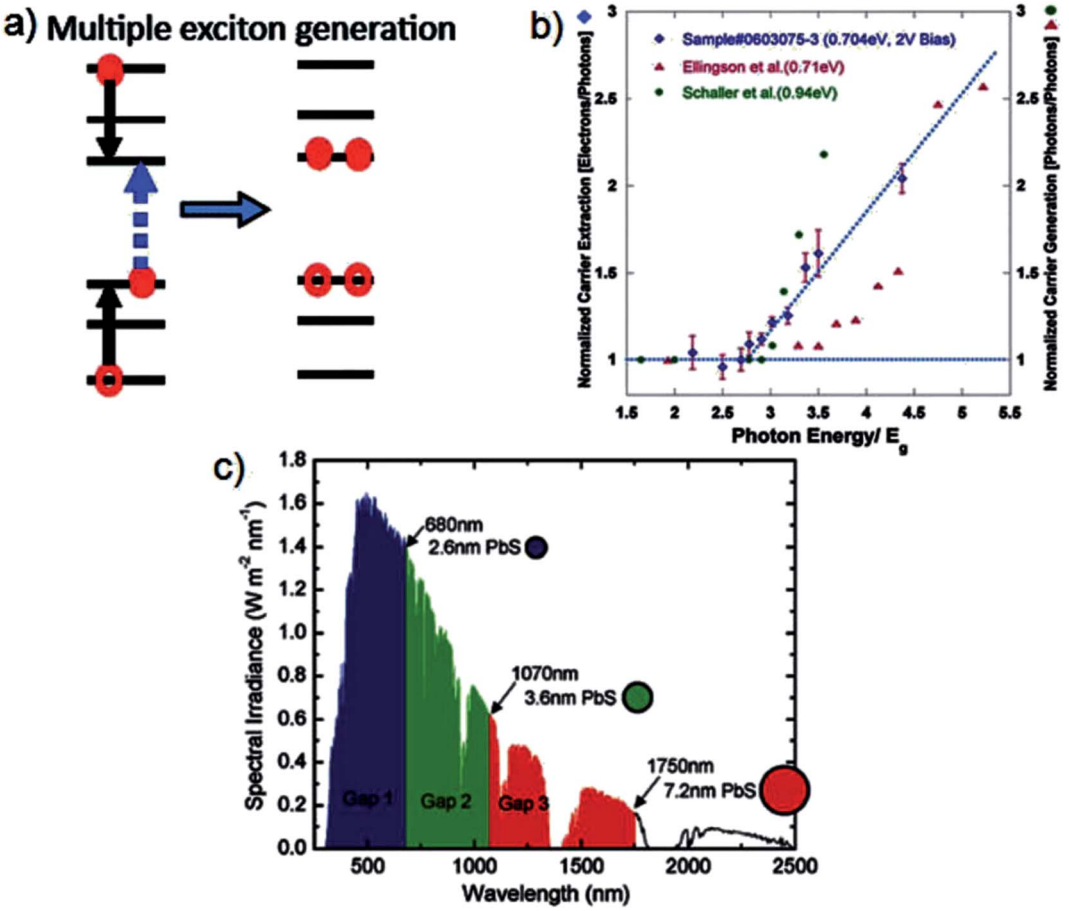

Fig. 2 (a) Schematic of multiple exciton generation.[11] (b) Extraction of excitons generated by MEG in a PbSe nanocrystal device.[12] (c) The concept of using IV–VI semiconductor PbS QDs with different sizes to build a triple-junction tandem solar cell, each absorbing in a different spectral range.[8]

review, we will primarily summarize the development of QDSCs over the recent five years.

1.2 The operational principle of QDSCs

The classical architecture of a QDSC consists of three components: a QD sensitized photoanode, a CE and, a redox electrolyte having S^{2-}/S_n^{2-} couples, as shown in Fig. 4a.[20] The photoanode is fabricated by coating a mesoporous wide bandgap semiconductor layer (TiO_2, ZnO) with an optimal thickness of *ca.* 10 μm and a porosity of 50–60% on the conducting glass. Then, the QD photosensitizers are adsorbed onto the surface of mesoporous semiconductor nanostructures, leading to photon absorption and electron injection. As shown in Fig. 4b, when persistently irradiated by incident light, QDs can absorb photons and excite electrons from the valence band (VB) of QDs to their conduction band (CB). Due to the good match of energy levels, electrons are injected into the CB of TiO_2 (see reaction (1)), and then transferred along the percolating network of TiO_2 nanocrystallites to transparent conductive oxide (TCO) (see reaction (2)). QDs are subsequently regenerated by reducing species (see reaction (3)) in the electrolyte that acts as a hole-transport medium. Finally, holes are transported to the CE, where the oxidized counterpart of the redox system is reduced (see reaction (4)). A major force that counteracts these favorable processes (see reaction (1)–(4)) is the charge recombination of electrons in the conduction band of QDs and TiO_2 at the electrolyte interface (see reaction (5) and (6)).[21]

$$TiO_2/QD + h\nu \rightarrow TiO_2/QD\ (electron + hole) \rightarrow TiO_2\ (electron) + QD\ (hole) \quad (1)$$

$$TiO_2\ (electron) + TCO \rightarrow TiO_2 + TCO\ (electron) \quad (2)$$

$$S^{2-} + 2QD\ (hole) + S_{(n-1)}^{2-} \rightarrow S_n^{2-} + QD \quad (3)$$

$$S_n^{2-} + 2TCO\ (electron) \rightarrow S^{2-} + S_{(n-1)}^{2-} \quad (4)$$

$$2QD\ (electron) + S_n^{2-} \rightarrow S^{2-} + S_{(n-1)}^{2-} + QD \quad (5)$$

$$2TiO_2\ (electron) + S_n^{2-} \rightarrow S^{2-} + S_{(n-1)}^{2-} + TiO_2 \quad (6)$$

Several parameters have been employed to estimate the photovoltaic performances of QDSCs. According to photocurrent density–voltage (J–V) characteristics of the solar cell, the conversion efficiency (η) of the cells is obtained as follows:[8]

$$\eta(\%) = \frac{J_m \times V_m}{P} = \frac{J_{sc} \times V_{oc} \times FF}{P} \times 100\%$$

where V_{oc} is the open-circuit voltage, J_{sc} is the short-circuit current density, P is the incident solar power on the device, and FF is the fill factor. J_{sc} is the photocurrent density derived at zero bias voltage which is dependent on light intensity, light absorption, injection efficiency, and regeneration of QDs, while V_{oc} is the maximum voltage that a solar cell can generate which is determined by the difference between the Fermi level of the wide bandgap semiconductor and the redox potential of the redox system.[22,23]

2. Photoanodes in QDSCs

2.1 QD materials

With an aim to improve the photovoltaic performances of QDSCs, many researchers have focused their attention on materials selection and materials engineering. According to the above discussion, the energy level of QDs employed in QDSCs must match that of wide bandgap semiconductors. To the best of our knowledge, enormous literature studies have reported the availability of different QDs with an appropriate bandgap (as listed in Table 1) as photosensitizers in QDSCs including $CuInS_2$,[24] PbS,[25,26] InP,[27] InAs,[28] Bi_2S_3,[29] Ag_2S,[30,31] Ag_2Se,[32] CdS,[33–35] CdSe,[36,37] CdTe,[34,38,39] ZnSe,[40] graphene,[41] and Si.[42] Among them, Cd chalcogenide QDs are preferred as they are more stable in QDSCs although they may degrade upon visible illumination.[43]

2.2 Semiconductor films

Semiconductor films coated on the surface of wide bandgap semiconductors are key components within QDSC devices. In recent years, several approaches have been explored to improve the performance of QDSCs and some of the significant results

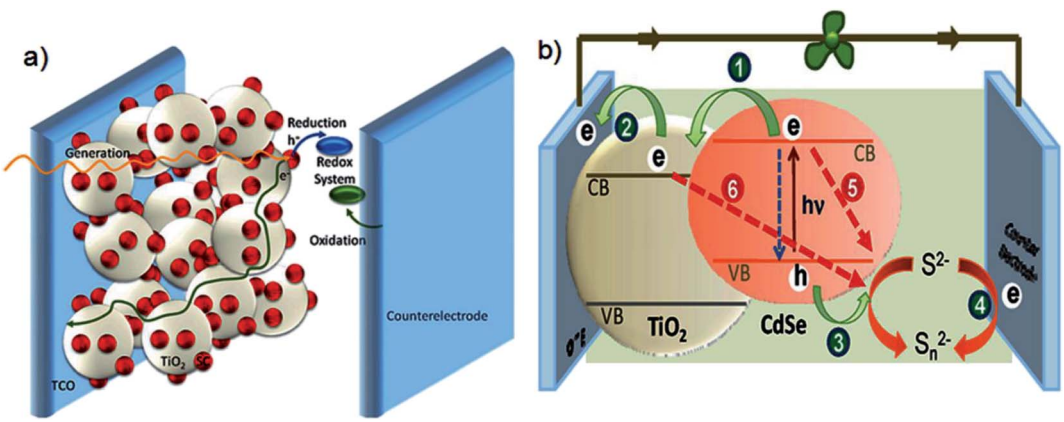

Fig. 4 (a) The general scheme of a typical QDSC device.[20] (b) Interfacial charge transfer processes that follow excitation of semiconductor nanocrystals in QDSCs.[21]

Table 1 Representative VB level (E_{VB}), CB level (E_{CB}) and bandgap energies (E_g) for narrow bandgap semiconductors

Materials	E_{VB} (eV)	E_{CB} (eV)	E_g (eV)
TiO_2	−7.3	−4.1	3.2
ZnO	−7.6	−4.2	3.4
CdS	−6.1	−3.7	2.4
CdSe	−6.0	−4.1	2.1
CdTe	−5.2	−3.7	1.5
PbS	−5.11	−4.74	0.37
ZnS	−7.1	−3.5	3.6
$CuInS_2$	−5.6	−4.1	1.5
In_2S_3	−5.7	−3.7	2.0
Ag_2S	−5.4	−4.5	0.9
InP	−5.3	−3.95	1.35
InAs	−5.3	−4.94	0.36
Graphene QDs	−6.1	−3.6	2.5

are summarized in Table 2 for quick and easy comparison among the QDSCs that have been reported. However, the conversion efficiencies are still lower than those of DSSCs. The major problems limiting the efficiency enhancement are attributed to insufficient light absorption, recombination of photoelectrons with holes in the electrolyte, and the slow charge transfer process between the CE and electrolyte.

A challenging topic for improving the conversion efficiency is to advance J_{sc} and V_{oc}. In order to increase the light absorption, the combination of different kinds of QDs with different bandgaps, expanding the absorption range within the solar spectrum, has been widely studied, and these integrated QD systems include CdS/CdSe,[59,78,79] CdS/PbS,[80] $CuInS_2$/CdS,[81] $CuInS_2/In_2S_3$,[55] CdSe/CdTe,[69] CdSe/GO,[82] *etc.* By appropriately matching the energy level of QDs, facile electron transfer is beneficial to the elevation of electron density on the photoanode and therefore J_{sc}. Among them, core/shell QD sensitizers with advanced structure and superior photoelectric properties are regarded as outstanding building blocks of QDSCs due to the enhanced charge injection efficiency and inhibited charge recombination process.[65,83,84] A highly efficient inverted type-I CdS/CdSe core/shell structure (see Fig. 5a) has been explored by Zhong *et al.*[67] With the narrower bandgap material grown epitaxially around the core of the wider bandgap material, the charge carriers (electrons and holes) are distributed largely in the shell region. Meanwhile, this favors the extraction of photogenerated electrons as well as holes and enhances the electron injection rate.[85] Ideal QD sensitizers should bear the characteristic of a wide absorption range, high CB edge, and free of trap-state defects. To further enhance V_{oc} and cell efficiency, type-II ZnTe/CdSe and CdTe/CdSe core/shell QDs have also been explored, as illustrated in Fig. 5b, yielding conversion efficiencies of 7.17% and 6.67%, respectively.[70] The prominent efficiency is attributed to the enhanced electron injection rate and the retarded charge recombination process because the shell can act as a tunneling barrier for the hole localized in the core. Furthermore, the augmentation of band offset and the stronger photo-induced dipole (PID) effect which brings forward an upward shift of the TiO_2 CB edge are other reasons resulting in the enhancement of the resultant cell devices. From Fig. 6, it can be seen that the PID effect can significantly increase the V_{oc} because photogenerated holes in type-II QDs are retained in the core for a relatively long time, allowing for the accumulation of a positively charged layer. Meanwhile, the electron injection to the CB of TiO_2 is favorable for the formation of a dipole moment.[86–88] This novel design strategy has the potential to improve the conversion efficiency of QDSC devices.

The performance of QDSC devices is seriously reduced by the recombination of photoelectrons with holes in the electrolyte as shown in Fig. 4b. How to suppress the loss of photoelectrons in the interface within the photoanode is an urgent requirement to improve the conversion efficiency. It is well known that

Table 2 Photovoltaic performances of recent QDSCs with different QDs[a]

QD photosensitizers	Wide bandgap semiconductors	CEs	η (%)	Ref.
CdS	TiO_2 microspheres	Pt	2.63	44
CdS	ZnO/TiO_2 nanosheets	CuS	1.95	45
CdS	ZnO pyramid arrays	Pt	1.60	46
CdSe	Porous TiO_2	Pt	2.23	47
CdSe	TiO_2	Cu_2S	3.70	48
CdTe	TiO_2	Pt	0.19	49
$Cu_{1.7}S$	TiO_2	Au	0.90	50
In_2S_3	TiO_2	Pt	1.30	51
InAs	TiO_2	Pt	0.30	28
Ag_2Se	TiO_2	Pt	1.76	32
PbS	TiO_2 nanotube arrays	Pt	3.41	52
$CuInS_2$	TiO_2	Cu_2S/RGO	2.51	53
$CuInSe_2$	TiO_2	Cu_2S	4.30	54
$CuInS_2/In_2S_3$	Mesoporous TiO_2	Cu_2S	1.62	55
$CuInS_2$/CdS	TiO_2 nanotubes	Pt	7.30	56
CdS/CdSe	Graphene/TiO_2	PbS	2.80	57
CdS/CdSe	ZnO nanorods–nanosheets	Cu_2S	3.28	58
CdS/CdSe	TiO_2	Cu_2S	4.05	59
CdS/CdSe	ZnO	Cu_2S	4.46	60
CdS/CdSe	ZnO nanoflowers	CuS	1.30	61
CdS/CdSe	TiO_2 spheres	Pt	4.81	18
CdTe/CdS	TiO_2	Cu_2S	2.44	39
CdSe/ZnSe/ZnS	TiO_2	Pt	3.46	62
CdS/CdSe/CdS/ZnS	TiO_2	Cu_2S	5.47	63
$Cu_2S/CuInS_2$/ZnSe	TiO_2	Pt	2.52	64
PbS/CdS core/shell	Mesoporous TiO_2	Cu_xS	1.28	65
$CdSe_xTe_{1-x}$/CdS core/shell	Mesoporous TiO_2	Cu_2S	5.04	66
CdS/CdSe core/shell	TiO_2	Cu_2S	5.32	67
$CuInS_2$/ZnS core/shell	Mesoporous TiO_2	Cu_2S	7.04	68
CdTe/CdSe core/shell	Mesoporous TiO_2	Cu_2S	6.76	69
ZnTe/CdSe core/shell	TiO_2	Cu_2S	7.17	70
$CdSe_xTe_{1-x}$	TiO_2	Cu_2S	6.36	71
CdS_xSe_{1-x}/Mn–CdS	TiO_2 nanotube arrays	CuS	3.26	72
Co–CdS/CdSe/ZnS	TiO_2	Cu_2S	3.16	73
Mn–CdS/CdSe	TiO_2	Cu_2S/GO	5.40	74
CdSe rods	TiO_2	PbS	2.70	75
ZnSe/CdSe/ZnSe	ZnO	Pt	6.20	76[b]
Perovskite QDs	TiO_2	Pt	6.50	77

[a] Electrolytes are aqueous solutions unless otherwise stated. [b] Polysulfide gel electrolyte.

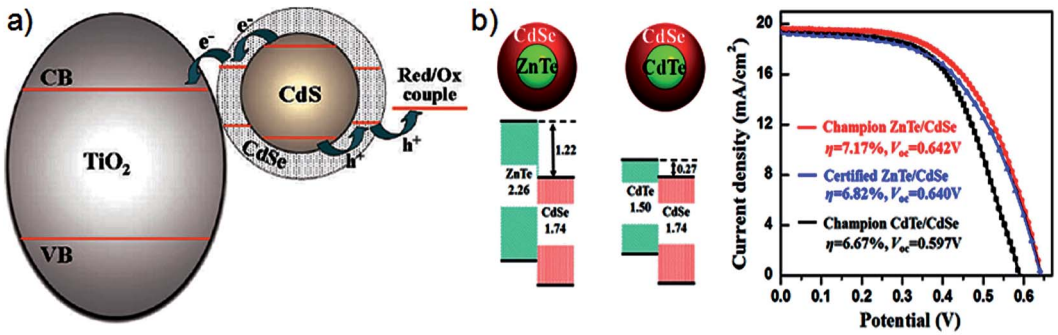

Fig. 5 Schematic diagram of the bandgap edge alignment of (a) the inverted type-I CdS/CdSe core/shell structure,[67] (b) the type-II ZnTe/CdSe and CdTe/CdSe core/shell structure and the *J*–*V* curves of the QDSCs.[70]

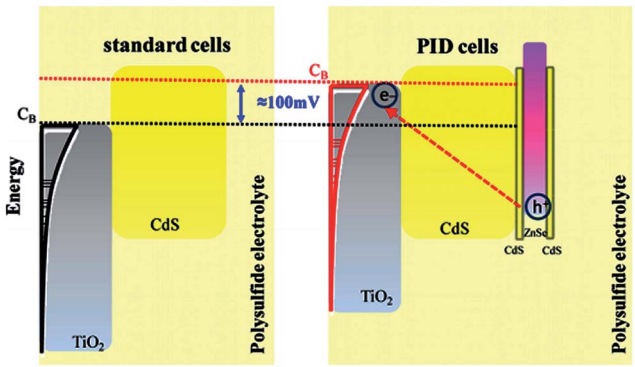

Fig. 6 Schematic presentation of the PID effect.[88]

enormous defect states on the surface of QDs are believed to be the primary reason for unsatisfactory J_{sc}, in this fashion, optimization of surface states and reduction in photoelectron loss are crucial to further enhance QDSC performances. Passivation of QDs, a high-efficiency strategy, has helped to significantly increase the efficiency of QDSCs by organic and inorganic passivating agents.[62,89,90] According to pre-treatment, the original trap states on the surface of the QDs can be reduced, leading to decreased recombination of charge carriers. Iván Mora-Seró's group has found that passivation strongly depends on the passivation agent, obtaining an enhancement of the solar cell efficiency for compounds containing amine and thiol groups, such as dimethylamine (DMA), ethylenediamine (ETDA), and ethanedithiol (EDT), as shown in Fig. 7. In contrast, the performance of devices can be decreased using passivating agents with acid groups such as thioglycolic acid (TGA) and formic acid (FA).[91] The distinction effect could be ascribed to the lower acidity coefficient (pK_a) of carboxylic groups on TGA and FA than those of alkylamine-(DMA and ETDA) and alkylthiol-(EDT). The corrosion and deactivation of QDs would be attributed to lower pK_a, resulting in partial loss of functionality. Moreover, amines can enhance the luminescence of semiconductor particles by reducing the nonradiative recombination, thus improving electron injection and finally photocurrent. Meanwhile, inorganic passivating agents, such as ZnS, ZnSe and halides, can also improve the performance of QDSC devices.[63,92–94] The combined ZnS/SiO_2 treatment on the $CdSe_xTe_{1-x}$ sensitized photoanode can significantly reduce interfacial recombination and increase charge collection efficiency, resulting in a certified record efficiency of 8.21%.[95] Besides, chemical surface treatment with those materials can induce a shift of the TiO_2 CB or a change in the recombination properties of electrons in TiO_2, producing a solidarity movement of the TiO_2 electron quasi-Fermi level which consequently results in a higher V_{oc}. Recently, a hybrid passivation strategy employing mercaptopropionic acid which can significantly increase the loading amount of quantum dots though the interaction

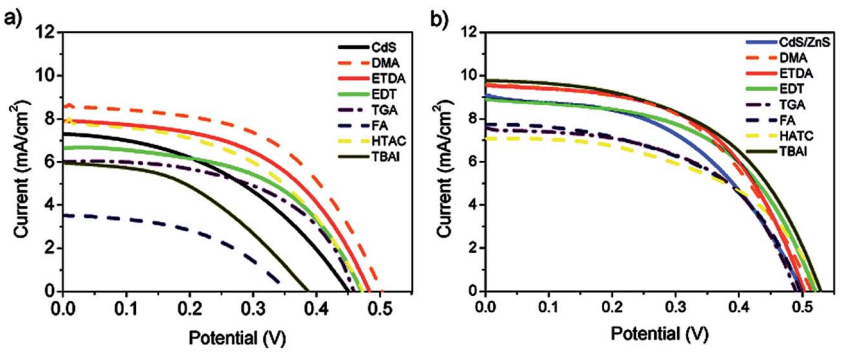

Fig. 7 *J*–*V* curves of the (a) CdS and (b) CdS/ZnS QDSCs treated with different organic and inorganic surface passivation agents.[91]

between –SH groups with QDs and TiO_2,[69,71] and importing iodide anions through tetrabutylammonium iodide to decrease the recombination loss has been explored, leading to a significant enhancement of the power conversion efficiency of QDSCs by 41%.[96] In short, in pursuit of excellent performance of QDSC devices, J_{sc} and V_{oc} can be significantly enhanced employing a passivation strategy, which provides a promising method to optimize the surface of QDs and bring QDSCs into the next big breakthrough in photovoltaics.

Additionally, the rapid electron transport along the percolating network from wide bandgap inorganic semiconductors (TiO_2, ZnO) has an accelerated effect on high cell performances by construction engineering. It is well understood that the wide bandgap semiconductor acts like a bridge to acquire the photoinject electron from the sensitizer and transfer the electron to fluorine-doped tin oxide (FTO).[62] Thus, expediting the electron flow rate from sensitizers to the substrate can efficiently reduce the backward reaction of electrons with the electrolyte. Based on this theory, great effort has been made on structuring fascinating geometry of wide bandgap semiconductors in recent years. From Fig. 8 and 9, polymorphic semiconductors, such as TiO_2 nanotube arrays,[72] nanorod arrays,[97,98] nanodendrite arrays,[99] nanowire/nanotube composites,[100] ZnO nanorod arrays,[101] nanosheets,[102] nanoflowers,[61] nanotube arrays, forests, and pyramid arrays,[46] have been sensitized with QDs and employed as photoanodes for QDSC devices. In 2007, Sun *et al.* reported photoanodes from CdS QD sensitized TiO_2 nanotube arrays, yielding a significant cell efficiency of 4.15% under AM 1.5 G illumination. This enhanced performance is attributed to the crystalline nature of the semiconductors and the film geometry allowing a fast and efficient transfer of the photogenerated electrons from QDs to the substrate, which compares favorably with the traditional mesoporous film electrodes leading to a much reduced electron–hole recombination and much improved photocurrent and efficiency.[35] Furthermore, single wall carbon nanotube/TiO_2 nanocomposites,[103] vertical nanosheet-structured ZnO/TiO_2,[45] and the vertically aligned hierarchical TiO_2 nanowire/ZnO nanorod or TiO_2 nanowire/ZnO nanosheet hybrid arrays[104] are also successfully synthesized and employed as photoanodes, yielding a conversion efficiency as high as 4.57% for CdS/CdSe based QDSCs. Besides, the improvement of electron transfer and separation rates along QDs should be also taken into consideration. In this fashion, engineering QD construction is essential to modify the properties of QDs. Considering the purpose to optimize the performance of QDSC devices, quantum rods were also deposited rapidly by electrophoresis onto mesoporous TiO_2 electrodes and photovoltaic efficiency values of up to 2.7% were measured for QRSCs.[75]

Apart from the strategies of employing polymorphic TiO_2 and ZnO, other approaches have been employed to improve the performance of QDSC devices. Doping optically active transition metal ions is an effective way to modify the electronic and photophysical properties of QDs because of the created electronic states in the midgap region of the QDs, thus altering the photogenerated electron separation and recombination dynamics. For example, Santra *et al.* succeeded in significantly

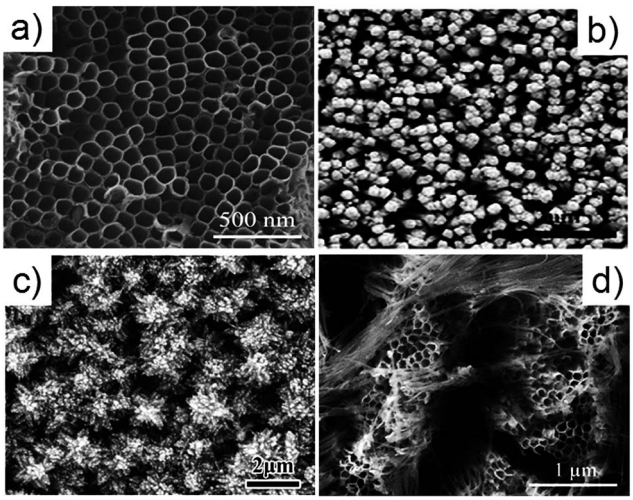

Fig. 8 The polymorphic TiO_2: (a) nanotube array,[72] (b) nanorod array,[97] (c) nanodendrite array,[99] and (d) nanowire/nanotube composite.[100]

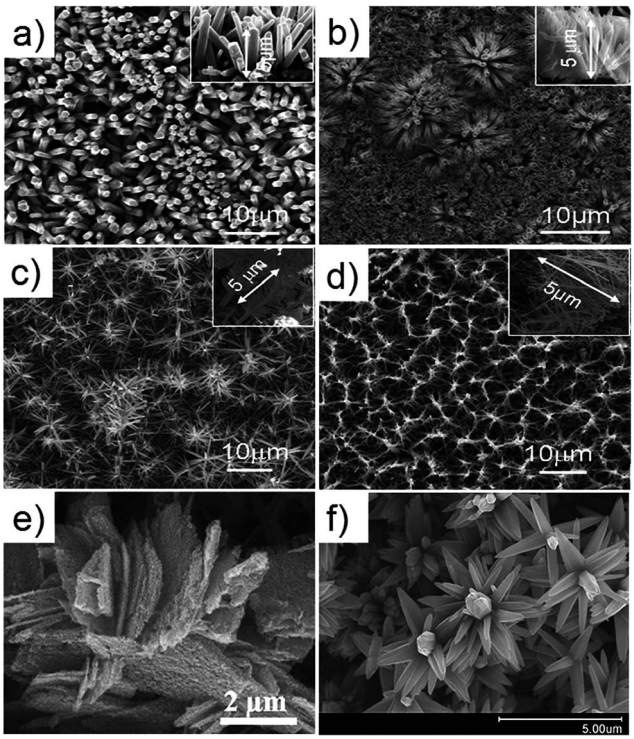

Fig. 9 The polymorphic ZnO: (a) nanorod array, (b) nanotube array, (c) forest, (d) pyramid array,[46] (e) nanosheets,[102] and (f) nanoflowers.[61]

improving the performance of QDSCs by employing the Mn^{2+} doping of CdS/CdSe.[74] The high conversion efficiency is mainly attributed to long-lived charge carriers in QD sensitizers introduced by the Mn^{2+} d–d transition as well as the enhanced ability to capture all incident photons. According to the discussion above, passivation of QDs can significantly advance the performance of QDSC devices. Likely, pre-treating the wide bandgap semiconductor is another approach to reduce electron recombination. A thin TiO_2-coating layer deposited onto a

nanocrystalline TiO_2 electrode by $TiCl_4$ gains an enhanced efficiency by 40% compared with a bare QDSC.[105] Consequently, the main contribution of all the approaches lies in the reduced recombination rate at the interface and the significantly suppressed charge recombination.

3. CEs in QDSCs

The task of a CE is to collect electrons from an external circuit and reduce the oxidized species (such as S_n^{2-} ions) to a reduced state, therefore the properties of the CE must be catalytically active toward the redox electrolyte. In a typical DSSC device, a Pt-based CE has been widely studied because of its high catalytic activity to reduce I_3^- to I^-.[106] However, Pt CEs are unsuitable for polysulfide electrolytes mainly because of their strong chemisorption with S^{2-}/S_n^{2-} couples (so-called poisoning effect), leading to a reduced chemical activity of the CE.[107,108] Meanwhile, the kinetics of charge transfer at the CE/electrolyte interface significantly affects the FF. Thus, exploration of the new materials with better catalytic activity and electrical conductivity to substitute Pt is an efficient strategy to improve the conversion efficiency of QDSCs, such as metal chalcogenides, carbon materials, and conducting polymers.

Recently, nanostructured metal chalcogenides such as CoS,[109] Co_9S_8,[110,111] NiS,[112] CuS,[113] $Cu_{1.8}S$,[114] Cu_2S,[115,116] CuSe,[117] FeS_2,[118] PbS,[108] Cu_2SnS_3,[119] and $Cu_2ZnSnSe_4$ (ref. 120–122) have been found to be cost-effective alternatives to Pt CEs. These compounds have superior catalytic activity towards the reduction of redox electrolytes due to weak inter-layer van der Waals forces.[123] Among them, the Cu_2S CE shows the highest electrocatalytic activity toward reduction of S_n^{2-} species in QDSCs.[70] The most simple preparation route is to directly immerse the metal foil substrate into sulfide solution to obtain an interfacial layer of metal sulfides. However, the CEs fabricated by this method can be continually corroded by the S^{2-}/S_n^{2-} electrolyte, resulting in the poisoning of the photocathode and detachment from substrates.[124] In order to solve this problem, ITO or FTO glass as a promising substrate for metal sulfide CEs has been explored. Furthermore, in order to increase the amount of metal sulfide, ITO@Cu_2S tunnel junction nanowire arrays as efficient CEs for QDSCs have been explored by Jiang *et al.*,[125] as shown in Fig. 10. The dedicatedly designed and fabricated core/shell nanowire array CEs significantly improve the charge collection and transport abilities as well as avoid the intrinsic issue of copper dissolution in popular and most efficient Cu/Cu_2S CEs. The power conversion efficiency of QDSCs with the designed ITO@Cu_2S CEs is increased by 33.5% in comparison with Cu/Cu_2S CE based solar cells. Meanwhile, the methods of electrochemical deposition,[126] CBD,[127] SILAR,[128] and thermal sulfidation of metal films[129] are also employed to construct the CEs on TCO glass. Zhao *et al.* prepared a Cu_2S film on the FTO glass substrate (Cu_2S/FTO) by electrodeposition of the copper film *via* a multipotential step technique followed by dipping into polysulfide methanol solution, and employed as CEs in CdSe QD sensitized solar cells, exhibiting a power conversion efficiency of 5.21% (see Fig. 11).[130] However, the charge carrier mobility is not significant in these CEs. Therefore, a challenge of optimizing the CE materials is to improve the conducting ability.

Apart from transition metal sulfides, carbonaceous materials have also received growing attention as CEs for QDSCs.[131] However, the relatively slow intrinsic reaction kinetics of carbon with the polysulfide electrolyte leads to the poor performance of QDSCs. By overcoming this problem of carbonaceous materials, some researchers have paid attention to fabricate carbon at an atomic level instead of the structural characteristics.[132,133] For example, the hollow core-mesoporous shell carbon (HCMSC) CE has been synthesized for QDSC applications, yielding a higher conversion efficiency than that based on conventional Pt.[134] The efficiency enhancement is attributed to the superior structural characteristics such as large specific surface area, high mesoporous volume, and particularly 3D interconnected unique hierarchical nanostructure of HCMSCs. Dong *et al.* utilized N-doped carbon nanoparticles as effective CE catalysts, and they found an enhanced electrocatalytic activity of N-doped carbon by the additional electrons provided by the nitrogen dopant atoms as well as the active sites.[133] Meanwhile, the combination of carbonaceous materials with metal chalcogenides is also considered as a facile strategy to improve the QDSC performance.[135,136] Carbonaceous materials with low sheet resistance, high charge carrier mobility and good corrosion

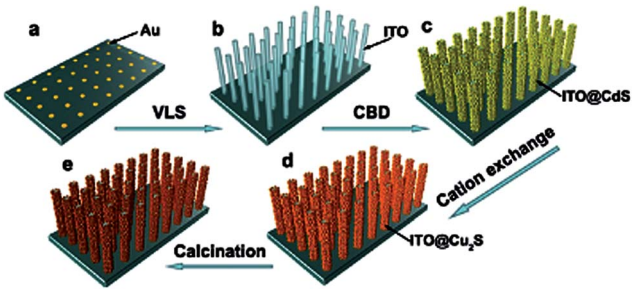

Fig. 10 Scheme for directly preparing ITO@Cu_2S nanowire arrays on FTO glass. (a) Sputtering Au catalysts on the FTO substrate; (b) chemical vapor deposition synthesis of ITO nanowire arrays; (c) CBD preparation of the CdS shell on ITO nanowire arrays; (d) cation exchange to form ITO@Cu_2S nanowire arrays; (e) calcination for improving the interfaces between the ITO nanowire core and Cu_2S nanocrystal shell.[125]

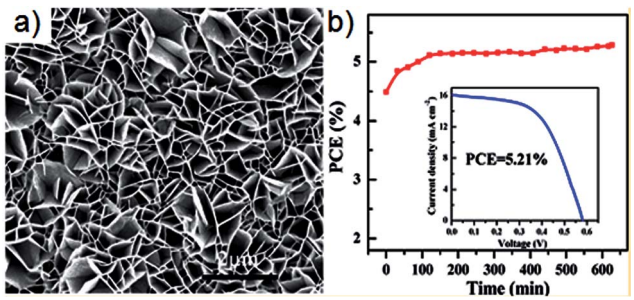

Fig. 11 (a) Top SEM image of the optimized Cu_2S/FTO CE. (b) *J*–*V* curve and stability of the QDSC with the CdSe QD sensitized photoanode and Cu_2S/FTO CE.[130]

resistance can be regarded as a conductive support and catalyst to load CE materials, such as graphene/PbS,[137] graphene/CoS,[138] carbon nanofiber/CuS,[139] multiwall carbon nanotube/$Cu_2ZnSnSe_4$,[140] carbon black/PbS,[141] and reduced graphene oxide/Cu_2S.[107] Water-soluble multiwall carbon nanotubes (MWCNTs) and $Cu_2ZnSnSe_4$ (CZTSe) nanoparticle composites were successfully synthesized by Zeng *et al.* and were employed as CEs for QDSCs, producing an efficiency of 4.60%.[140] The enhanced electrocatalytic properties of the composited CE materials arise from the improved charge transport rate to the active catalyst sites in the CE in coordination with carbon, illustrated in Fig. 12. The electrons from the external circuit are delivered to the CZTSe catalyst along the MWCNT and are used to reduce the oxidized polysulfide electrolyte (see Fig. 12a). Within this reaction process, the CZTSe plays a critical role whereas the MWCNT provides an excellent path for electron transfer rapidly due to the outstanding electron conductivity of the MWCNT. Moreover, the combination of carbon nanotubes and graphene provides a greatly enlarged surface area; this allows an increased amount of metal chalcogenide catalysts. With further optimization, carbon derived materials would be promising candidates for CE materials because of their competitive prices and good electrocatalytic properties in comparison to other types of CEs.

Conducting polymers such as polyaniline (PANI), poly(3,4-ethylenedioxythiophene) (PEDOT), and polypyrrole (PPy) have been widely utilized as CEs in DSSCs.[142–144] Due to their high electron conductivity, low cost-availability, and large electrochemical surface area, the conducting polymers can also be used as CEs in QDSCs. In 2011, Yeh *et al.* prepared CEs using conducting polymers [PEDOT, PPy and polythiophene (PT)],[145] generating efficiencies of 1.35%, 0.09%, and 0.41% for the solar cells with PEDOT, PT, and PPy CEs, respectively. The authors demonstrated that the promising efficiency of the cell with the PEDOT electrode is attributed to higher electrocatalytic activity, reduced charge transfer resistance at the CE/electrolyte interface, and the higher porosity and surface roughness of the PEDOT film.

Although the reported efficiencies of QDSCs are still lower than those of other solar cells, breakthroughs in QDSCs will be realized with further studies to improve the electrocatalytic ability of CEs.

4. Electrolytes

The recent research in the utilization of semiconductor QDs for solar energy conversion has provided a promising alternative concept to conventional photovoltaic devices. The common electrolytes used in DSSCs are organic electrolytes containing an I^-/I_3^- redox couple.[146–150] Unfortunately, the I^-/I_3^- redox couple is corrosive to most quantum dots, leading to degradation of QDSC performance.[151] Thus, exploring an appropriate iodine-free electrolyte is critical for stable QDSCs. The sulfide/polysulfide (S^{2-}/S_n^{2-}) redox couple in the aqueous electrolyte provides a stable environment for QDs. However, the QDSCs employing the S^{2-}/S_n^{2-} redox couple with higher redox potential generate low V_{oc} and very poor FF. Recently, a new electrolyte of the Co^{2+}/Co^{3+} redox system is used to improve the V_{oc} due to the relative low redox potential in comparison to the S^{2-}/S_n^{2-} redox couple, whereas the photocurrents are still lower than that of the S^{2-}/S_n^{2-} redox couple.[152] Besides, Fe^{2+}/Fe^{3+} and $Fe(CN)_6^{5-}/Fe(CN)_6^{4-}$ redox systems are also investigated in CdS-sensitized solar cells.[153] Until now, the QDSCs employing the S^{2-}/S_n^{2-} redox couple have shown the highest efficiency.[95] The FF and V_{oc} should be further increased by selecting an appropriate electrolyte, such as replacing the S^{2-}/S_n^{2-} redox couple with $[(CH_3)_4N]_2S/[(CH_3)_4N]_2S_n$ in an organic solvent, yielding an impressive V_{oc} of 1.2 V.[154]

Great achievements have been made on QDSCs, but the long-term stability is also important in realizing the commercialization of QDSCs. Volatilization of the liquid electrolyte and permeation of water or oxygen molecules lead to the rapid degradation of performance during the operation of the device. By addressing this issue, an effective approach to solve such a problem is by replacing the volatile liquid electrolyte with quasi-solid-state or solid-state electrolytes.[155,156]

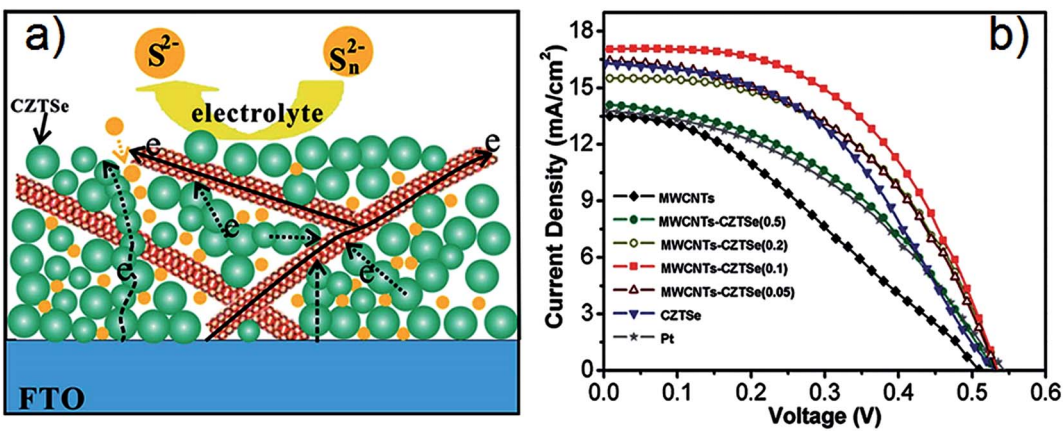

Fig. 12 (a) Schematic of the suggested "composite charge transmission" model for the MWCNT–CZTSe composite CEs in a QDSC system. (b) Characteristic *J*–*V* curves for the QDSCs with Pt, MWCNT, CZTSe, and MWCNT–CZTSe composite CEs.[140]

The quasi-solid-state polymer gel electrolyte shows high ionic conductivity, good thermal stability and favorable penetration ability into nanocrystalline porous TiO_2 films, thus it has been widely used in DSSCs.[157,158] In general, the liquid electrolyte is trapped in the network to form a homogeneous quasi-solid-state electrolyte. Yu *et al.* first used the chemically crosslinked polyacrylamide-based hydrogel as the polymer matrix to prepare the quasi-solid-state polysulfide electrolyte for CdS/CdSe co-sensitized solar cells and 4.0% of the efficiency was achieved.[159] As we all know, the liquid electrolyte can be easily trapped into a three-dimensional (3D) gel matrix by the osmotic pressure. In our previous work, aiming at accelerating the reduction reaction of redox species, conducting polymers (PANI and PPy)[160] and carbonaceous materials (graphene, graphene oxide)[161] have been incorporated into the gel systems to fabricate conducting gel electrolytes. Conducting polymer gel electrolytes by incorporating graphene into the 3D polyacrylamide matrix was also successfully prepared and employed to assemble CdS sensitized solar cells.[162] The electrocatalytic reaction was expanded from the CE/electrolyte interface to both the interface and the gel electrolyte, resulting in the increased performance. Furthermore, in order to increase the amount of liquid electrolyte loading, the synergistic effect of both osmotic pressure and capillary force is believed to be an effective strategy to further elevate the dosage of the liquid electrolyte in per unit volume of the gel electrolyte. Thus, the dense matrices were freeze-dried after swollen in deionized water. The conversion efficiency of the device was enhanced to 2.34% in comparison to 1.36% for pure polymer gel electrolyte based solar cells. Meanwhile, a low molecular mass gelator, such as dextran, 12-hydroxystearic acid and a natural polysaccharide Konjac glucomannan based highly conductive hydrogel polysulfide electrolyte have been developed,[163–165] and the enhanced stability was shown in Fig. 13. The good permeation and high conductivity of the gel electrolyte, in which the electron transport is even much faster than the liquid electrolyte, may be the main reason for its excellent photovoltaic performance. At the same time, the good intrinsic stability of the hydrogel electrolyte contributes to the long-term stability.

For further increasing the stability of QDSCs, solid-state electrolytes and hole conductors have been used to replace liquid electrolytes and quasi-solid-state electrolytes in QDSCs.

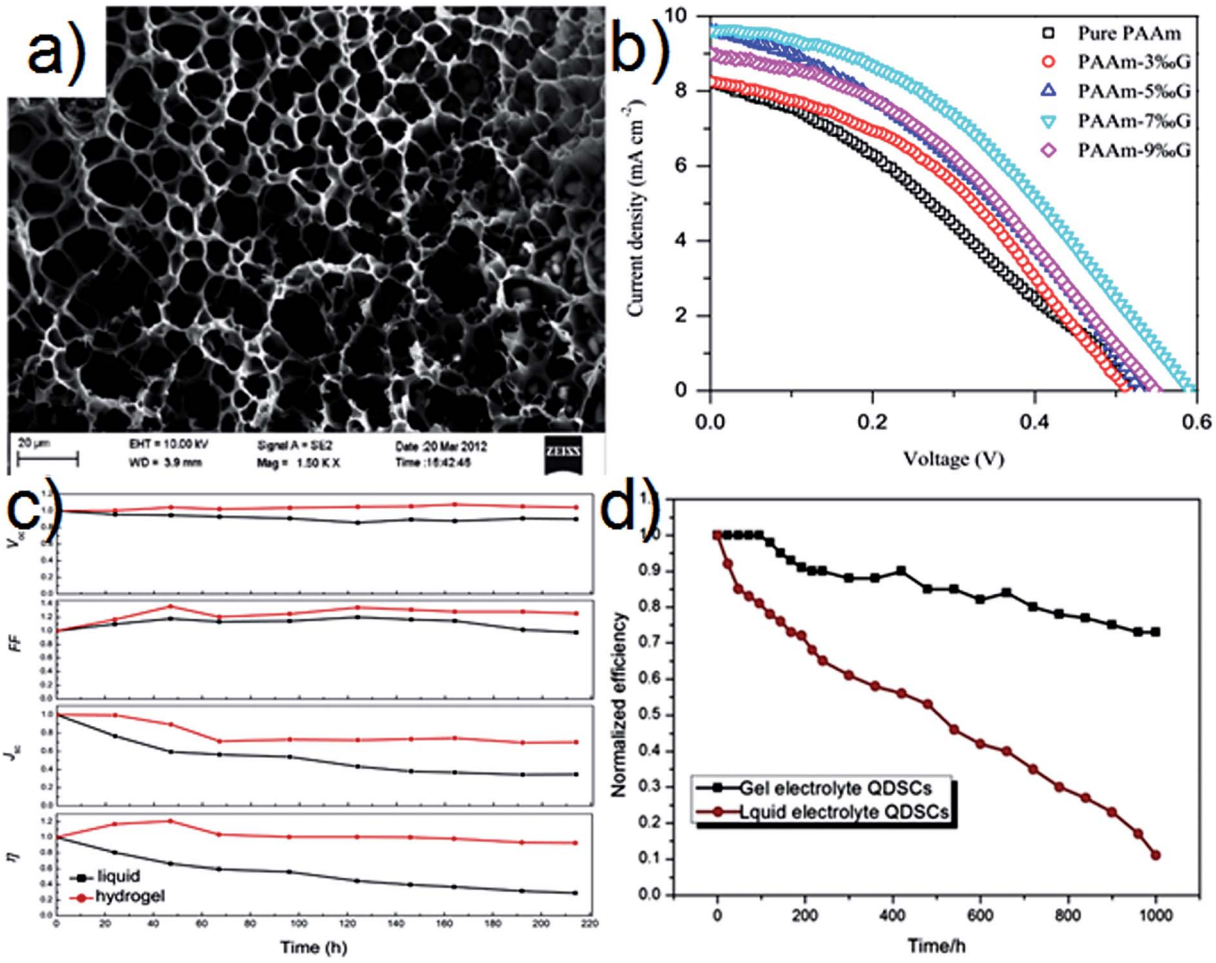

Fig. 13 (a) SEM image of the microporous crosslinked polyacrylamide matrix. (b) *J*–*V* characteristics of quasi-solid-state QDSCs with conducting gel electrolytes.[162] (c) Normalized device performance variation with the QDSCs based on the liquid electrolyte and hydrogel electrolyte at 60 °C.[164] (d) Time-course change of the normalized efficiencies for the QDSCs with the gel electrolyte and liquid electrolyte.[165]

However, the conversion efficiency of QDSCs based on solid-state electrolytes is lower than the solar cell devices with liquid electrolytes. The main reasons for unsatisfactory photovoltaic behavior can be attributed to the weak penetration ability of polymer solid-state electrolytes into mesoporous TiO_2 films as well as the relatively inferior electron conductivity, which limits the film thickness of the solid electrolyte and lowers the light harvesting efficiency. Thus, a crucial factor to advance the efficiency is to improve the conductivity and penetration ability of the electrolyte. Recently, solid-state electrolytes based on poly(ethylene oxide)–poly(vinylidene fluoride) polymer blends with a S/tetramethylammonium sulfate (S/TMAS) redox additive were investigated.[166] The study showed that the PEO–PVDF polymer electrolyte with the S/TMAS redox additive could improve the solar cell incident photon-to-current conversion efficiency and stability. A similar discovery was reported by adding sodium sulfide (Na_2S) to the solid-state electrolyte.[167] The created polysulfide ions, S_n^{2-}, serving as the electron scavenger at the electrolyte/counter electrode interface and S^{2-} consuming holes at the photoanode/electrolyte interface within the solid electrolyte are the crucial compounds to enhance the properties of the solid electrolyte. Meanwhile, it is confirmed that the ionic conductivity of the electrolyte with additives such as Na_2S is significantly modified. In our previous study, we have synthesized a class of solid polymer electrolytes based on polyvinylpyrrolidone (PVP).[168] An optimized conversion efficiency of 0.55% is measured for the QDSCs employing the PVP/$10Na_2S$–S solid electrolyte. Although the conversion efficiency is still lower than that of liquid electrolyte based QDSCs, the work demonstrated the feasibility of designing cost-effective solid-state electrolytes with polymers and redox species as additives. However, the exploration of solid electrolytes based on polymers for solid-state QDSCs is still limited because of low penetration ability and unsatisfactory conductivity. By addressing this issue, a plastic crystal based solid-state electrolyte composed of plastic crystal succinonitrile and Na_2S was creatively synthesized by a simple blending approach.[169] Owing to the significantly enhanced conductivity, an optimal power conversion efficiency of 1.29% is measured. The results demonstrate that exploring a new medium to substitute the polymer gives the possibility to prepare a superior solid-state electrolyte. Another promising approach of fabricating solid-state electrolytes for QDSCs is to employ p-type semiconductors, such as CuSCN,[170] 2,2′,7,7′-tetrakis(*N*,*N*-di-*p*-methoxyphenylamine)9,9′-spirobifluorene (spiro-OMeTAD),[171] and poly(3-hexyl thiophene) (P3HT).[172] Although the research on all-solid-state electrolytes for QDSC applications is in a primary stage, the promising peculiarity will trigger researchers to still explore more efficient and stable QDSC materials and devices.

5. Summary and perspective

QDSCs have become a promising alternative for DSSCs due to the excellent properties of QD photosensitizers. High power conversion efficiency can be achieved through high-energy photon excitation. However, the relatively low power conversion efficiency is still not comparable to other photovoltaic devices. The factors that limit the efficiency of QDSCs include limited absorption of incident light, recombination at the anode/electrolyte and the low FF arising from unsatisfactory CE performances. By addressing these issues, optimizing the construction of QD sensitizers, CEs with superior catalytic activity and redox couple electrolyte can improve the performance of QDSCs. Combination of diversified inorganic semiconductor QDs and passivation of QDs by organic and inorganic passivating agents can enhance the light absorption and electron excitation and reduce the recombination at the interface. Among them, the type-II core/shell structure can significantly increase the V_{oc} arising from PID effects. On the other hand, highly ordered architectures of wide bandgap semiconductors provide fast and efficient transfer of photogenerated electrons from QDs to the substrate.

Owing to the distinction between QDSCs and DSSCs in redox couples, the electrocatalytic ability of Pt is not satisfactory, leading to a low FF. Metal chalcogenides, carbon materials, conducting polymers, and carbon material/metal chalcogenide composites are explored and employed in QDSCs. Although there have been some efforts to utilize conducting polymers, the resultant PCEs of QDSCs employing these CEs are not high. By combining the advantages of carbon materials (high conductivity) and metal chalcogenides (high catalytic ability), the advanced performance of CEs has been achieved. Apart from improving the conversion efficiency, long-term stability is necessary to be taken into account. Generally, polymer gel electrolytes and solid-state hole conductors as quasi-state and solid-state electrolytes are utilized in QDSCs. However, the properties of these QDSCs employing quasi-state electrolytes and solid-state electrolytes are still poorer than that of those based on liquid electrolytes.

In conclusion, for further development, future studies should focus on improving the QDSC performance. For example, the design of new semiconductor QDs to broaden the absorption spectral region offers a range of new opportunities and challenges to improve the efficiency. Moreover, deeper research on surface treatment provides a new strategy to reduce the recombination. Also, further studies of CEs with high electrocatalytic ability are expected to be the breakthrough in the currently stagnant research field of QDSCs. Much attention might be paid on the stability of QDSCs, in which the weak penetration ability of polymer electrolytes and inferior electron conductivity limit the development. It is expected that exploring highly efficient solid-state solar cells will be a persistent objective in the near future.

Acknowledgements

The authors would like to acknowledge financial support from the Fundamental Research Funds for the Central Universities (201313001, 201312005), Shandong Province Outstanding Youth Scientist Foundation Plan (BS2013CL015), Shandong Provincial Natural Science Foundation (ZR2011BQ017), Research Project for the Application Foundation in Qingdao (13-4-198-jch), National Natural Science Foundation of China

(51102219, 51342008, U1037604), National Key and National Key Technology Support Program (2012BAB15B02).

References

1 J. P. Holdren, *Science*, 2008, **319**, 424.
2 M. Grätzel, R. A. J. Janssen, D. B. Mitzi and E. H. Sargent, *Nature*, 2012, **488**, 304.
3 B. O'Regan and M. Grätzel, *Nature*, 1991, **353**, 737.
4 S. Mathew, A. Yella, P. Gao, R. Humphry-Baker, B. F. E. Curchod, N. Ashari-Astani, I. Tavernelli, U. Rothlisberger, M. K. Nazeeruddin and M. Grätzel, *Nat. Chem.*, 2014, **6**, 242.
5 S. Gorer and G. Hodes, *J. Phys. Chem.*, 1994, **98**, 5338.
6 W. W. Yu, L. Qu, W. Guo and X. Peng, *Chem. Mater.*, 2003, **15**, 2854.
7 R. D. Schaller, V. M. Agranovich and V. I. Klimov, *Nat. Phys.*, 2005, **1**, 189.
8 J. Tang and E. H. Sargent, *Adv. Mater.*, 2011, **23**, 12.
9 E. H. Sargent, *Nat. Photonics*, 2009, **3**, 325.
10 M. C. Hanna and A. J. Nozik, *J. Appl. Phys.*, 2006, **100**, 074510.
11 M. T. Trinh, L. Polak, J. M. Schins, A. J. Houtepen, R. Vaxenburg, G. I. Maikov, G. Grinbom, A. G. Midgett, J. M. Luther, M. C. Beard, A. J. Nozik, M. Bonn, E. Lifshitz and L. D. A. Siebbeles, *Nano Lett.*, 2011, **11**, 1623.
12 S. J. Kim, W. J. Kim, Y. Sahoo, A. N. Cartwright and P. N. Prasad, *Appl. Phys. Lett.*, 2008, **92**, 031107.
13 H. Lee, M. Wang, P. Chen, D. R. Gamelin, S. M. Zakeeruddin, M. Grätzel and M. K. Nazeeruddin, *Nano Lett.*, 2009, **9**, 4221.
14 G. Zhu, L. Pan, T. Xu and Z. Sun, *ACS Appl. Mater. Interfaces*, 2011, **3**, 1472.
15 I. Robel, V. Subramanian, M. Kuno and P. V. Kamat, Quantum Dot Solar Cells, *J. Am. Chem. Soc.*, 2006, **128**, 2385.
16 B. J. M. Luther, J. Gao, M. T. Lloyd, O. E. Semonin, M. C. Beard and A. J. Nozik, *Adv. Mater.*, 2010, **22**, 3704.
17 N. P. Benehkohal, V. González-Pedro, P. P. Boix, S. Chavhan, R. Tena-Zaera, G. P. Demopoulos and I. Mora-Seró, *J. Phys. Chem. C*, 2012, **116**, 16391.
18 X. Y. Yu, J. Y. Liao, K. Q. Qiu, D. B. Kuang and C. Y. Su, *ACS Nano*, 2011, **5**, 9494.
19 P. V. Kamat, *J. Phys. Chem. Lett.*, 2013, **4**, 908.
20 I. Mora-Seró and J. Bisquert, *J. Phys. Chem. Lett.*, 2010, **1**, 3046.
21 P. V. Kamat, *Acc. Chem. Res.*, 2012, **45**, 1906.
22 G. Y. Chen, J. Seo, C. H. Yang and P. N. Prasad, *Chem. Soc. Rev.*, 2013, **42**, 8304.
23 A. Fukui, N. Fuke, R. Komiya, N. Koide, R. Yamanaka, H. Katayama and L. Y. Han, *Appl. Phys. Express*, 2009, **2**, 082202.
24 J. Y. Chang, S. C. Chang, S. H. Tzing and C. H. Li, *ACS Appl. Mater. Interfaces*, 2014, **6**, 22272.
25 S. D. Sung, I. Lim, P. Kang, C. Lee and W. I. Lee, *Chem. Commun.*, 2013, **49**, 6054.
26 X. N. Li, W. H. Lu, Y. N. Wang, Y. Y. Fang, L. L. Wang, Q. L. Ai, X. W. Zhou and Y. Lin, *Electrochim. Acta*, 2014, **144**, 71.
27 A. Zaban, O. I. Micic, B. A. Gregg and A. J. Nozik, *Langmuir*, 1998, **14**, 3153.
28 P. Yu, K. Zhu, A. G. Norman, S. Ferrere, A. J. Frank and A. J. Nozik, *J. Phys. Chem. B*, 2006, **110**, 25451.
29 I. Zumeta-Dubé, V. F. Ruiz-Ruiz, D. Díaz, S. Rodil-Posadas and A. Zeinert, *J. Phys. Chem. C*, 2014, **118**, 11495.
30 A. Tubtimtaea, K. Wua, H. Tung, M. Lee and G. Wang, *Electrochem. Commun.*, 2010, **12**, 1158.
31 C. Chen, Y. Xie, G. Ali, S. H. Yoo and S. O. Cho, *Nanoscale Res. Lett.*, 2011, **6**, 462.
32 A. Tubtimtae, M. Lee and G. Wang, *J. Power Sources*, 2011, **196**, 6603.
33 E. Guo, L. Yin and L. Zhang, *CrystEngComm*, 2014, **16**, 3403.
34 J. H. Bang and P. V. Kamat, *ACS Nano*, 2009, **3**, 1467.
35 W. T. Sun, Y. Yu, H. Y. Pan, X. F. Gao, Q. Chen and L. M. Peng, *J. Am. Chem. Soc.*, 1124, **130**.
36 K. Wang, W. W. He, L. Wu, G. P. Xu, S. L. Ji and C. H. Ye, *RSC Adv.*, 2014, **4**, 15702.
37 N. Fuke, L. B. Hoch, A. Y. Koposov, V. W. Manner, D. J. Werder, A. Fukui, N. Koide, H. Katayama and M. Sykora, *ACS Nano*, 2010, **4**, 6377.
38 X. F. Gao, H. B. Li, W. T. Sun, Q. Chen, F. Q. Tang and L. M. Peng, *J. Phys. Chem. C*, 2009, **113**, 7531.
39 X. H. Shen, J. G. Jia, Y. Lin and X. W. Zhou, *J. Power Sources*, 2015, **277**, 215.
40 Z. J. Ning, H. N. Tian, C. Z. Yuan, Y. Fu, H. Y. Qin, L. C. Sun and H. Ågren, *Chem. Commun.*, 2011, **47**, 1536.
41 X. Yan, X. Cui, B. Li and L. S. Li, *Nano Lett.*, 2010, **10**, 1869.
42 G. Uchida, M. Sato, H. Seo, K. Kamataki, N. Itagaki, K. Koga and M. Shiratani, *Thin Solid Films*, 2013, **544**, 93.
43 A. G. Kontos, V. Likodimos, E. Vassalou, I. Kapogianni, Y. S. Raptis, C. Raptis and P. Falaras, *Nanoscale Res. Lett.*, 2011, **6**, 266.
44 Y. Zhang, S. Lin, W. Zhang, Y. Zhang, F. Y. Qi, S. Y. Wu, Q. Pei, T. Feng and X. M. Song, *Electrochim. Acta*, 2014, **150**, 167.
45 S. J. Li, Z. Chen, T. Li, H. P. Gao, C. C. Wei, W. Li, W. P. Kong and W. F. Zhang, *Electrochim. Acta*, 2014, **127**, 362.
46 Y. Zhao, H. Y. Guo, H. Hua, Y. Xi and C. G. Hu, *Electrochim. Acta*, 2014, **115**, 487.
47 X. H. Song, M. Q. Wang, T. Y. Xing, J. P. Deng, J. J. Ding, Z. Yang and X. Y. Zhang, *J. Power Sources*, 2014, **253**, 17.
48 B. Gao, C. Shen, S. L. Yuan, B. Zhang, M. Y. Zhang, Y. X. Yang and G. R. Chen, *J. Alloys Compd.*, 2014, **612**, 323.
49 A. Badawi, N. Al-Hosiny, S. Abdallah, S. Negm and H. Talaat, *Sol. Energy*, 2013, **88**, 137.
50 M. C. Lin and M. W. Lee, *Electrochem. Commun.*, 2011, **13**, 1376.
51 J. L. Duan, Q. W. Tang, B. L. He and L. M. Yu, *Electrochim. Acta*, 2014, **139**, 381.
52 L. Tao, Y. Xiong, H. Liu and W. Z. Shen, *Nanoscale*, 2014, **6**, 931.
53 D. H. Jara, S. J. Yoon, K. G. Stamplecoskie and P. V. Kamat, *Chem. Mater.*, 2014, **26**, 7221.
54 J. Yang, J. Y. Kim, J. H. Yu, T. Y. Ahn, H. Lee, T. S. Choi, Y. W. Kim, J. Joo, M. J. Ko and T. Hyeon, *Phys. Chem. Chem. Phys.*, 2013, **15**, 20517.

55 Y. Q. Wang, Y. C. Rui, Q. H. Zhang, Y. G. Li and H. Z. Wang, *ACS Appl. Mater. Interfaces*, 2013, **5**, 11858.
56 C. Chen, G. Ali, S. H. Yoo, J. M. Kum and S. O. Cho, *J. Mater. Chem.*, 2011, **21**, 16430.
57 L. Chen, L. Tuo, J. Rao and X. F. Zhou, *Mater. Lett.*, 2014, **124**, 161.
58 J. J. Tian, E. Uchaker, Q. F. Zhang and G. Z. Cao, *ACS Appl. Mater. Interfaces*, 2014, **6**, 4466.
59 R. Zhou, Q. F. Zhang, E. Uchaker, J. Lan, M. Yin and G. Z. Cao, *J. Mater. Chem. A*, 2014, **2**, 2517.
60 C. H. Li, L. Yang, J. Y. Xiao, Y. C. Wu, M. Søndergaard, Y. H. Luo, D. M. Li, Q. B. Meng and B. B. Iversen, *Phys. Chem. Chem. Phys.*, 2013, **15**, 8710.
61 S. K. Kim, S. Park, M. K. Son and H. J. Kim, *Electrochim. Acta*, 2015, **151**, 531.
62 C. M. Liu, L. L. Mu, J. G. Jia, X. W. Zhou and Y. Lin, *Electrochim. Acta*, 2013, **111**, 179.
63 L. L. Mu, C. M. Liu, J. G. Jia, X. W. Zhou and Y. Lin, *J. Mater. Chem. A*, 2013, **1**, 8353.
64 J. Y. Chang, L. F. Su, C. H. Li, C. C. Chang and J. M. Lin, *Chem. Commun.*, 2012, **48**, 4848.
65 L. H. Lai, L. Protesescu, M. V. Kovalenko and M. A. Loi, *Phys. Chem. Chem. Phys.*, 2014, **16**, 736.
66 J. H. Luo, H. Y. Wei, F. Li, Q. L. Huang, D. M. Li, Y. H. Luo and Q. B. Meng, *Chem. Commun.*, 2014, **50**, 3464.
67 Z. X. Pan, H. Zhang, K. Cheng, Y. M. Hou, J. L. Hua and X. H. Zhong, *ACS Nano*, 2012, **6**, 3982.
68 Z. X. Pan, I. Mora-Seró, Q. Shen, H. Zhang, Y. Li, K. Zhao, J. Wang, X. H. Zhong and J. Bisquert, *J. Am. Chem. Soc.*, 2014, **136**, 9203.
69 J. Wang, I. Mora-Seró, Z. X. Pan, K. Zhao, H. Zhang, Y. Y. Feng, G. Yang, X. H. Zhong and J. Bisquert, *J. Am. Chem. Soc.*, 2013, **135**, 15913.
70 S. Jiao, Q. Shen, I. Mora-Seró, J. Wang, Z. X. Pan, K. Zhao, Y. Kuga, X. H. Zhong and J. Bisquert, *ACS Nano*, 2015, **9**, 908.
71 Z. X. Pan, K. Zhao, J. Wang, H. Zhang, Y. Y. Feng and X. H. Zhong, *ACS Nano*, 2013, **7**, 5215.
72 Z. Li, L. B. Yu, Y. B. Liu and S. Q. Sun, *Electrochim. Acta*, 2015, **153**, 200.
73 N. Firoozi, H. Dehghani and M. Afrooz, *J. Power Sources*, 2015, **278**, 98.
74 P. K. Santra and P. V. Kamat, *J. Am. Chem. Soc.*, 2012, **134**, 2508.
75 A. Salant, M. Shalom, Z. Tachan, S. Buhbut, A. Zaban and U. Banin, *Nano Lett.*, 2012, **12**, 2095.
76 K. Yan, L. Zhang, J. Qiu, Y. Qiu, Z. Zhu, J. Wang and S. Yang, *J. Am. Chem. Soc.*, 2013, **135**, 9531.
77 J. H. Im, C. R. Lee, J. W. Lee, S. W. Park and N. G. Park, *Nanoscale*, 2011, **3**, 4088.
78 J. J. Tian, Q. F. Zhang, E. Uchaker, Z. Q. Liang, R. Gao, X. H. Qu, S. G. Zhang and G. Z. Cao, *J. Mater. Chem. A*, 2013, **1**, 6770.
79 B. Y. L. Lee and Y. S. Lo, *Adv. Funct. Mater.*, 2009, **19**, 604.
80 V. González-Pedro, C. Sima, G. Marzari, P. P. Boix, S. Giménez, Q. Shen, T. Dittrichf and I. Mora-Seró, *Phys. Chem. Chem. Phys.*, 2013, **15**, 13835.
81 J. H. Luo, H. Y. Wei, Q. L. Huang, X. Hu, H. F. Zhao, R. Yu, D. M. Li, Y. H. Luo and Q. B. Meng, *Chem. Commun.*, 2013, **49**, 3881.
82 I. V. Lightcap and P. V. Kamat, *J. Am. Chem. Soc.*, 2012, **134**, 7109.
83 W. J. Li and X. H. Zhong, *J. Phys. Chem. Lett.*, 2015, **6**, 796.
84 H. M. Zhu, N. H. Song and T. Q. Lian, *J. Am. Chem. Soc.*, 2010, **132**, 15038.
85 Z. Ning, H. Tian, H. Qin, Q. Zhang, H. Ågren, L. Sun and Y. Fu, *J. Phys. Chem. C*, 2010, **114**, 15184.
86 J. M. Azpiroz, E. Ronca and F. D. Angelis, *J. Phys. Chem. Lett.*, 2015, **6**, 1423.
87 M. Kazes, S. Buhbut, S. Itzhakov, O. Lahad, A. Zaban and D. Oron, *J. Phys. Chem. Lett.*, 2014, **5**, 2717.
88 S. Buhbut, S. Itzhakov, I. Hod, D. Oron and A. Zaban, *Nano Lett.*, 2013, **13**, 4456.
89 P. Ardalan, T. P. Brennan, H. B. R. Lee, J. R. Bakke, I. K. Ding, M. L. D. McGehee and S. F. Bent, *ACS Nano*, 2011, **5**, 1495.
90 A. Tubtimtae and M. W. Lee, *Thin Solid Films*, 2015, **526**, 225.
91 M. S. Fuente, R. S. Sánchez, V. González-Pedro, P. P. Boix, S. G. Mhaisalkar, M. E. Rincón, J. Bisquert and I. Mora-Seró, *J. Phys. Chem. Lett.*, 2013, **4**, 1519.
92 R. Ahmed, L. Zhao, A. J. Mozer, G. Will, J. Bell and H. X. Wang, *J. Phys. Chem. C*, 2015, **119**, 2297.
93 J. Tang, K. W. Kemp, S. Hoogland, K. S. Jeong, H. Liu, L. Levina, M. Furukawa, X. Wang, R. Debnath, D. Cha, K. W. Chou, A. Fischer, A. Amassian, J. B. Asbury and E. H. Sargent, *Nat. Mater.*, 2011, **10**, 765.
94 Z. Y. Peng, Y. L. Liu, Y. H. Zhao, K. Q. Chen, Y. Q. Cheng, V. Kovalev and W. Chen, *J. Alloys Compd.*, 2014, **587**, 613.
95 K. Zhao, Z. X. Pan, I. Mora-Seró, E. Cánovas, H. Wang, Y. Song, X. Q. Gong, J. Wang, M. Bonn, J. Bisquert and X. H. Zhong, *J. Am. Chem. Soc.*, 2015, **137**, 5602.
96 J. Huang, B. Xu, C. Z. Yuan, H. Chen, J. L. Sun, L. C. Sun and H. Ågren, *ACS Appl. Mater. Interfaces*, 2014, **6**, 18808.
97 J. Jiao, Z. J. Zhou, W. H. Zhou and S. X. Wu, *Mater. Sci. Semicond. Process.*, 2013, **16**, 435.
98 C. Chen, M. Ye, M. Lv, C. Gong, W. Guo and C. Lin, *Electrochim. Acta*, 2014, **121**, 175.
99 Z. Y. Peng, Y. L. Liu, Y. H. Zhao, W. Shu, K. Q. Chen, Q. L. Bao and W. Chen, *Electrochim. Acta*, 2013, **111**, 755.
100 Z. Li, L. B. Yu, Y. B. Liu and S. Q. Sun, *Electrochim. Acta*, 2014, **129**, 379.
101 C. J. Raj, S. N. Karthick, S. Park, K. V. Hemalatha, S. K. Kim, K. Prabakar and H. J. Kim, *J. Power Sources*, 2014, **248**, 439.
102 H. N. Chen, W. P. Li, H. C. Liu and L. Q. Zhu, *Electrochem. Commun.*, 2011, **13**, 331.
103 A. Badawi, N. Al-Hosiny, S. Abdallah, A. Merazga and H. Talaat, *Mater. Sci. Semicond. Process.*, 2014, **26**, 162.
104 H. L. Feng, W. Q. Wu, H. S. Rao, Q. Wan, L. B. Li, D. B. Kuang and C. Y. Su, *ACS Appl. Mater. Interfaces*, 2015, **7**, 5199.
105 J. Kim, H. Choi, C. Nahm, C. Kim, S. Nam, S. Kang, D. R. Jung, J. I. Kim, J. Kang and B. Park, *J. Power Sources*, 2012, **220**, 108.

106 Y. Y. Duan, Q. W. Tang, J. Liu, B. L. He and L. M. Yu, *Angew. Chem., Int. Ed.*, 2014, **53**, 14569.
107 J. G. Radich, R. Dwyer and P. V. Kamat, *J. Phys. Chem. Lett.*, 2011, **2**, 2453.
108 Z. Tachan, M. Shalom, I. Hod, S. Rühle, S. Tirosh and A. Zaban, *J. Phys. Chem. C*, 2011, **115**, 6162.
109 Z. Yang, C. Y. Chen, C. W. Liu and H. T. Chang, *Chem. Commun.*, 2010, **46**, 5485.
110 W. Guo, C. Chen, M. Ye, M. Lv and C. Lin, *Nanoscale*, 2014, **6**, 3656.
111 C. Chen, M. Ye, N. Zhang, X. Wen, D. Zheng and C. Lin, *J. Mater. Chem. A*, 2015, **3**, 6311.
112 H. J. Kim, T. B. Yeo, S. K. Kim, S. S. Rao, A. D. Savariraj, K. Prabakar and C. V. V. M. Gopi, *Eur. J. Inorg. Chem.*, 2014, **2014**, 4281.
113 W. J. Ke, G. J. Fang, H. W. Lei, P. L. Qin, H. Tao, W. Zeng, J. Wang and X. Z. Zhao, *J. Power Sources*, 2014, **248**, 809.
114 M. Ye, X. Wen, N. Zhang, W. Guo, X. Liu and C. Lin, *J. Mater. Chem. A*, 2015, **3**, 9595.
115 G. S. Selopal, I. Concina, R. Milan, M. M. Natile, G. Sberveglieri and A. Vomiero, *Nano Energy*, 2014, **6**, 200.
116 M. Ye, C. Chen, N. Zhang, X. Wen, W. Guo and C. Lin, *Adv. Energy Mater.*, 2014, DOI: 10.1002/aenm.201301564.
117 F. Bo, C. F. Zhang, C. L. Wang, S. H. Xu, Z. Y. Wang and Y. P. Cui, *J. Mater. Chem. A*, 2014, **2**, 14585.
118 J. Xu, H. T. Xue, X. Yang, H. X. Wei, W. Y. Li, Z. P. Li, W. J. Zhang and C. S. Lee, *Small*, 2014, **10**, 4754.
119 C. Lee, J. Xu, X. Yang and T. L. Wong, *Nanoscale*, 2012, **4**, 6537.
120 X. W. Zeng, W. J. Zhang, Y. Xie, D. H. Xiong, W. Chen, X. B. Xu, M. K. Wang and Y. B. Cheng, *J. Power Sources*, 2013, **226**, 359.
121 Y. R. Zhang, C. W. Shi, X. Y. Dai, F. Liu, X. Q. Fang and J. Zhu, *Electrochim. Acta*, 2014, **118**, 41.
122 J. Xu, X. Yang, Q. D. Yang, T. L. Wong and C. S. Lee, *J. Phys. Chem. C*, 2012, **116**, 19718.
123 C. Li, L. Huang, G. P. Snigdha, Y. Yu and L. Cao, *ACS Nano*, 2012, **6**, 8868.
124 G. Hodes, J. Manassen and D. Cahen, *J. Electrochem. Soc.*, 1980, **127**, 544.
125 Y. Jiang, X. Zhang, Q. Q. Ge, B. B. Yu, Y. G. Zou, W. J. Jiang, W. G. Song, L. J. Wan and J. S. Hu, *Nano Lett.*, 2014, **14**, 365.
126 F. F. Wang, H. Dong, J. L. Pan, J. J. Li, Q. Li and D. S. Xu, *J. Phys. Chem. C*, 2014, **118**, 19589.
127 C. S. Kim, S. H. Choi and J. H. Bang, *ACS Appl. Mater. Interfaces*, 2014, **6**, 22078.
128 H. N. Chen, L. Q. Zhu, H. C. Liu and W. P. Li, *J. Phys. Chem. C*, 2013, **117**, 3739.
129 M. S. Faber, K. Park, M. Cabán-Acevedo, P. K. Santra and S. Jin, *J. Phys. Chem. Lett.*, 2013, **4**, 1843.
130 K. Zhao, H. J. Yu, H. Zhang and X. H. Zhong, *J. Phys. Chem. C*, 2014, **118**, 5683.
131 B. Z. Fang, M. Kim, S. Q. Fan, J. H. Kim, D. P. Wilkinson, J. Ko and J. S. Yu, *J. Mater. Chem.*, 2011, **21**, 8742.
132 M. Seol, E. Ramasamy, J. Lee and K. Yong, *J. Phys. Chem. C*, 2011, **115**, 22018.
133 J. H. Dong, S. P. Jia, J. Z. Chen, B. Li, J. F. Zheng, J. H. Zhao, Z. J. Wang and Z. P. Zhu, *J. Mater. Chem.*, 2012, **22**, 9745.
134 G. S. Paul, J. H. Kim, M. S. Kim, K. Do, J. Ko and J. S. Yu, *ACS Appl. Mater. Interfaces*, 2012, **4**, 375.
135 M. Seol, D. H. Youn, J. Y. Kim, J. W. Jang, M. Choi, J. S. Lee and K. Yong, *Adv. Energy Mater.*, 2013, DOI: 10.1002/aenm.201300775.
136 D. M. Li, L. Y. Cheng, Y. D. Zhang, Q. X. Zhang, X. M. Huang, Y. H. Luo and Q. B. Meng, *Sol. Energy Mater. Sol. Cells*, 2014, **120**, 454.
137 P. Parand, M. Samadpour, A. Esfandiar and A. I. Zad, *ACS Photonics*, 2014, **1**, 323.
138 H. W. Hu, J. N. Ding, J. F. Qian, Y. Li, L. Bai and N. Y. Yuan, *Mater. Lett.*, 2014, **114**, 7.
139 L. L. Li, P. N. Zhu, S. J. Peng, M. Srinivasan, Q. Y. Yan, A. S. Nair, B. Liu and S. Samakrishna, *J. Phys. Chem. C*, 2014, **118**, 16526.
140 X. W. Zeng, D. H. Xiong, W. J. Zhang, L. Q. Ming, Z. Xu, Z. F. Huang, M. K. Wang, W. Chen and Y. B. Cheng, *Nanoscale*, 2013, **5**, 6992.
141 Y. Y. Yang, L. F. Zhu, H. C. Sun, X. M. Huang, Y. H. Luo, D. M. Li and Q. B. Meng, *ACS Appl. Mater. Interfaces*, 2012, **4**, 6162.
142 Q. D. Tai, B. Chen, F. Guo, S. Xu, H. Hu, B. Sebo and X. Z. Zhao, *ACS Nano*, 2011, **5**, 3795.
143 R. Trevisan, M. Döbbelin, P. P. Boix, E. M. Barea, R. Tena-Zaera, I. Mora-Seró and J. Bisquert, *Adv. Energy Mater.*, 2011, **1**, 781.
144 S. S. Jeon, C. Kim, J. Ko and S. S. Im, *J. Mater. Chem.*, 2011, **21**, 8146.
145 M. H. Yeh, C. P. Lee, C. Y. Chou, L. Y. Lin, H. Y. Wei, C. W. Chu, R. Vittal and K. C. Ho, *Electrochim. Acta*, 2011, **57**, 277.
146 Q. W. Tang, H. Y. Cai, S. S. Yuan and X. Wang, *J. Mater. Chem. A*, 2013, **1**, 317.
147 B. L. He, Q. W. Tang, T. L. Liang and Q. H. Li, *J. Mater. Chem. A*, 2014, **2**, 3119.
148 Y. Y. Duan, Q. W. Tang, Z. H. Chen, B. L. He and H. Y. Chen, *J. Mater. Chem. A*, 2014, **2**, 12459.
149 H. Y. Cai, Q. W. Tang, B. L. He and P. J. Li, *J. Power Sources*, 2014, **258**, 117.
150 X. X. Chen, Q. W. Tang, B. L. He, L. Lin and L. M. Yu, *Angew. Chem., Int. Ed.*, 2014, **53**, 10799.
151 Y. L. Lee and C. H. Chang, *J. Power Sources*, 2008, **185**, 584.
152 S. Y. Chae, Y. J. Hwang and O. S. Joo, *RSC Adv.*, 2014, **4**, 26907.
153 Y. Tachibana, H. Y. Akiyama, Y. Ohtsuka, T. Torimoto and S. Kuwabata, *Chem. Lett.*, 2007, **36**, 88.
154 L. Li, X. C. Yang, J. J. Gao, H. N. Tian, J. Z. Zhao, A. Hagfeldt and L. C. Sun, *J. Am. Chem. Soc.*, 2011, **133**, 8458.
155 H. Kim, I. Hwang and K. Yong, *ACS Appl. Mater. Interfaces*, 2014, **6**, 11245.
156 C. Herzog, A. Belaidi, A. Ogacho and T. Dittrich, *Energy Environ. Sci.*, 2009, **2**, 962.
157 P. Wang, S. M. Zakeeruddin, J. E. Moser, M. K. Nazeeruddin, T. Sekiguchi and M. Grätzel, *Nat. Mater.*, 2003, **2**, 402.

158 S. H. Park, I. Y. Song, J. Lim, Y. S. Kwon, J. Choi, S. Song, J. R. Lee and T. Park, *Energy Environ. Sci.*, 2013, **6**, 1559.
159 Z. X. Yu, Q. X. Zhang, D. Qin, Y. H. Luo, D. M. Li, Q. Shen, T. Toyoda and Q. B. Meng, *Electrochem. Commun.*, 2010, **12**, 1776.
160 S. S. Yuan, Q. W. Tang, B. L. He and P. Z. Yang, *J. Power Sources*, 2014, **254**, 98.
161 S. S. Yuan, Q. W. Tang, B. L. He and Y. Zhao, *J. Power Sources*, 2014, **260**, 225.
162 J. L. Duan, Q. W. Tang, R. Li, B. L. He, L. M. Yu and P. Z. Yang, *J. Power Sources*, 2015, **284**, 369.
163 H. Y. Chen, L. Lin, X. Y. Yu, K. Q. Qiu, X. Y. Lü, D. B. Kuang and C. Y. Su, *Electrochim. Acta*, 2013, **92**, 117.
164 Z. P. Huo, L. Tao, S. M. Wang, J. F. Wei, J. Zhu, W. W. Dong, F. Liu, S. H. Chen, B. Zhang and S. Y. Dai, *J. Power Sources*, 2015, **284**, 582.
165 S. Wang, Q. X. Zhang, Y. Z. Xu, D. M. Li, Y. H. Luo and Q. B. Meng, *J. Power Sources*, 2013, **224**, 152.
166 Y. Yang and W. Y. Wang, *J. Power Sources*, 2015, **285**, 70.
167 G. Sfyri, S. Sfaelou, K. S. Andrikopoulos, N. Balis, G. A. Voyiatzis and P. Lianos, *J. Phys. Chem. C*, 2014, **118**, 16547.
168 J. L. Duan, Q. W. Tang, Y. N. Sun, B. L. He and H. Y. Chen, *RSC Adv.*, 2014, **4**, 60478.
169 J. L. Duan, Q. W. Tang, B. L. He and H. Y. Chen, *RSC Adv.*, 2015, **5**, 33463.
170 B. C. Lévy-Clément, R. Tena-Zaera, M. A. Ryan, A. Katty and G. Hodes, *Adv. Mater.*, 2005, **17**, 1512.
171 B. H. Lee, H. C. Leventis, S. J. Moon, P. Chen, S. Ito, S. A. Haque, T. Torres, F. Nüesch, T. Geiger, S. M. Zakeeruddin, M. Grätzel and M. K. Nazeeruddin, *Adv. Funct. Mater.*, 2009, **19**, 2735.
172 J. A. Chang, J. H. Rhee, S. H. Im, Y. H. Lee, H. Kim, S. I. Seok, M. K. Nazeeruddin and M. Grätzel, *Nano Lett.*, 2010, **10**, 2609.

